Plant roots use a patterning mechanism to position lateral root branches toward available water

Yun Bao[a,b,c], Pooja Aggarwal[b,1], Neil E. Robbins II[a,d,1], Craig J. Sturrock[e], Mark C. Thompson[e], Han Qi Tan[b], Cliff Tham[b], Lina Duan[a], Pedro L. Rodriguez[f], Teva Vernoux[g], Sacha J. Mooney[e], Malcolm J. Bennett[e,h], and José R. Dinneny[a,b,c,2]

[a]Department of Plant Biology, Carnegie Institution for Science, Stanford, CA 94305; [b]Temasek Lifesciences Laboratory, National University of Singapore, Singapore 117604; [c]Department of Biological Sciences, National University of Singapore, Singapore 117543; [d]Department of Biology, Stanford University, Stanford, CA 94305; [e]School of Biosciences, University of Nottingham, Loughborough LE12 5RD, United Kingdom; [f]Instituto de Biologia Molecular y Celular de Plantas, Consejo Superior de Investigaciones Científicas–Universitat Politécnica de Valéncia, ES-46022 Valencia, Spain; [g]Laboratoire de Reproduction et Développement des Plantes, Centre National de la Recherche Scientifique, Institut National de la Recherche Agronomique, École Normale Supérieure de Lyon, Université Claude Bernard de Lyon, Université de Lyon, F-69364 Lyon Cedex 07, France; and [h]College of Science, King Saud University, Riyadh 11451, Kingdom of Saudi Arabia

Edited by Maarten J. Chrispeels, University of California, San Diego, La Jolla, CA, and approved May 14, 2014 (received for review January 17, 2014)

The architecture of the branched root system of plants is a major determinant of vigor. Water availability is known to impact root physiology and growth; however, the spatial scale at which this stimulus influences root architecture is poorly understood. Here we reveal that differences in the availability of water across the circumferential axis of the root create spatial cues that determine the position of lateral root branches. We show that roots of several plant species can distinguish between a wet surface and air environments and that this also impacts the patterning of root hairs, anthocyanins, and aerenchyma in a phenomenon we describe as hydropatterning. This environmental response is distinct from a touch response and requires available water to induce lateral roots along a contacted surface. X-ray microscale computed tomography and 3D reconstruction of soil-grown root systems demonstrate that such responses also occur under physiologically relevant conditions. Using early-stage lateral root markers, we show that hydropatterning acts before the initiation stage and likely determines the circumferential position at which lateral root founder cells are specified. Hydropatterning is independent of endogenous abscisic acid signaling, distinguishing it from a classic water-stress response. Higher water availability induces the biosynthesis and transport of the lateral root-inductive signal auxin through local regulation of TRYPTOPHAN AMINOTRANSFERASE OF *ARABIDOPSIS* 1 and PIN-FORMED 3, both of which are necessary for normal hydropatterning. Our work suggests that water availability is sensed and interpreted at the suborgan level and locally patterns a wide variety of developmental processes in the root.

moisture regulation | root development | root system architecture | adaptive root response | auxin-regulated root patterning

The root system of plants is a branched network whose architecture is determined by endogenous and environmental cues and serves as a model for pattern formation (1). In *Arabidopsis*, lateral roots (LRs) are initially specified as founder cells (FCs) within the internal pericycle cell layer of the primary root (2). A temporally oscillating transcriptional network that results in periodic fluctuations in auxin response controls the patterning of FCs along the longitudinal axis of the primary root (3, 4). Moments of peak auxin response are maintained in fixed positions termed prebranch sites (PBS), which mark presumptive FCs and can be visualized using the *ProDR5:LUC+* reporter (4). In *Arabidopsis*, LRs only develop from pericycle cells that overlie one of the two xylem poles (5). Although two such populations of cells exist along the circumferential axis of the root, pericycle cells adjacent to only one xylem pole will be selected. How the xylem pole is chosen and whether environmental stimuli affect this process is currently unclear.

We report that when roots are grown vertically on the surface of an agar medium, LRs predominantly form on the side of the primary root that contacts agar. Through our developmental analysis, we show that the local environment impacts LR patterning by providing spatial cues that select one of the two xylem poles at which LR FCs will be specified. We observe this patterning phenomenon in all flowering plant species examined and also in a realistic soil environment. Because this phenomenon is elicited by exposing roots to an asymmetric distribution of available water, we have termed the process "hydropatterning."

Results

Patterning of Root Tissues Is Determined by the Local Availability of Water. Soil is a heterogeneous environment containing particles and aggregated structures of different sizes with pockets of air and nonuniform distributions of water and nutrients (6). Our understanding of how roots sense and interpret microscale heterogeneity is poor due, in part, to a lack of model experimental systems for studying such phenomena. Interestingly, growing *Arabidopsis* seedling roots along the surface of an agar medium creates spatial asymmetries in the environment the primary root is exposed to, but the effect of these differences has not been explored before. Under these conditions, one side of the primary root is in contact with the agar medium and the film of water that forms on its surface (contact side), whereas the other side of the primary root is exposed to air in the headspace of the Petri dish (air side) (Fig. 1*A*). We found that seedlings grown on agar media infrequently developed LRs that grew straight out into the

Significance

Few studies have asked at what spatial scale environmental stimuli regulate plant development and when during the patterning process these signals act. We have discovered that plant roots can sense microscale heterogeneity in water availability across their circumference, which causes dramatic differences in the patterning of tissues along this axis. Root branching is a target of such hydropatterning; lateral roots only form on the side of the main root contacting water in soil or agar. We show that hydropatterning is a conserved process in *Arabidopsis*, maize, and rice and reveal the importance of auxin biosynthesis and transport in regulating this process.

Author contributions: Y.B., P.A., N.E.R., C.J.S., H.Q.T., C.T., L.D., S.J.M., M.J.B., and J.R.D. designed research; Y.B., P.A., N.E.R., C.J.S., M.C.T., H.Q.T., C.T., L.D., and J.R.D. performed research; P.L.R. and T.V. contributed new reagents/analytic tools; Y.B., P.A., N.E.R., C.J.S., M.C.T., H.Q.T., C.T., L.D., and J.R.D. analyzed data; and Y.B., N.E.R., C.J.S., S.J.M., M.J.B., and J.R.D. wrote the paper.

The authors declare no conflict of interest.

This article is a PNAS Direct Submission.

Freely available online through the PNAS open access option.

[1]P.A. and N.E.R. contributed equally to this work.

[2]To whom correspondence should be addressed. E-mail: jdinneny@carnegiescience.edu.

This article contains supporting information online at www.pnas.org/lookup/suppl/doi:10.1073/pnas.1400966111/-/DCSupplemental.

air, suggesting that their patterning might be influenced by this environmental asymmetry (Fig. 1 *B*, *C*, and *D*). We created a phenotyping key to quantify the emergence patterns of LRs across the circumferential axis by categorizing emerged LRs as air side, horizon side, or contact side (*SI Appendix, SI Materials and Methods*, provides a full description of criteria used). Although we would have a priori expected that the chance of an LR emerging from any particular side of the primary root would be nearly equivalent, we instead observed a strong bias in LR emergence toward the contact side (Fig. 1*D*). This bias was lost when roots were grown through agar (Fig. 1 *A* and *D*), indicating

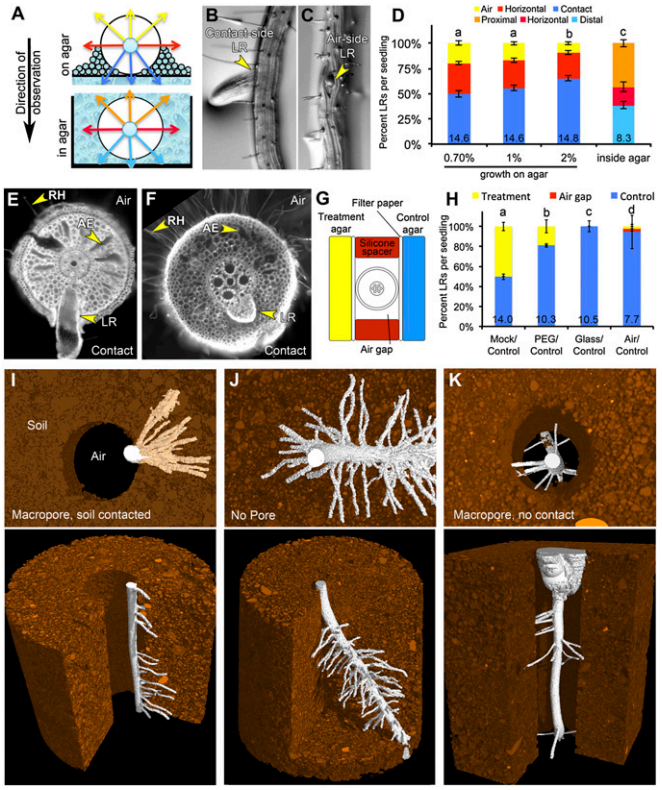

Fig. 1. Hydropatterning of root development in *Arabidopsis*, maize and rice. (*A*) Diagram showing asymmetries in the local environment generated when seedlings grow on the surface of an agar-based media or the symmetric environment generated when roots are grown through agar. (*B* and *C*) LR primordia emerging from the contact (*B*) or air side (*C*) of the primary root. (*D*) Quantification of LR emergence patterns from the primary root under different conditions ($n > 10$). Various phenotypic categories are indicated with different colors and are marked in *A*. (*E*) Cross-section of a rice primary root grown on agar, stained with calcofluor. Image shows the development of aerenchyma (AE) and root hairs (RH) on the air side and an LR emerging from the contact side. (*F*) Cross-section of a maize root grown on agar and stained with propidium iodide. (*G*) Diagram showing the construction of "agar sandwiches" used to test the effects of local differences in media composition on LR development in maize. (*H*) LR outgrowth is induced on two sides by contact with agar (Mock/Control); this effect is diminished on the "Treatment" side when the water potential of the media is reduced using PEG infusion (PEG/Control). Contact of the root with a glass surface does not induce LR outgrowth (Glass/Control). Growth of roots along a single agar surface results in the suppression of LR development on the air side (Air/Control) ($n > 10$). (*I*–*K*) MicroCT-generated images of maize seedlings grown through a macropore of air (*I* and *K*) or a continuous volume of soil (*J*). The root in *K* is growing in air, whereas in *I* the root is contacting the soil surface. Root tissue is false-colored in white, and soil is false-colored in brown. Average number of LRs per seedling (*D*) and per centimeter of primary root (*H*) is shown at base of columns in bar charts. Error bars indicate SEM. Significant differences based on Fisher's exact test ($P < 0.05$) with similar groups are indicated using the same letter.

that the observed phenomenon requires an asymmetric environment. Root curvature influences at which side of the root (concave or convex) a LR will initiate (3). We found that inducing a 90-degree bend in the root through gravitropic stimulation had no significant influence on the bias in LR development that occurred along the air–agar axis suggesting that these two processes act independently on the distribution of LRs (*SI Appendix*, Fig. S1).

Changing agar concentration in the growth media from 1 to 2% decreased water potential (Ψ_w) and the amount of expressed water on the surface of the media, which reduced the circumferential area of the root contacting liquid water (*SI Appendix*, Fig. S1) (7). This change in media composition also significantly affected the bias in the distribution of LRs (Fig. 1*D*). Use of different growth substrates indicated that no specific component of the media besides water was necessary to elicit biased LR development, although these media differed significantly in water potential (range, −0.22 MPa) (*SI Appendix*, Fig. S2). These data suggest that contact with water, in or on the surface of the media, had a greater influence on the local induction of LR development than small differences in water potential.

Growth of *Oryza sativa* (rice) and *Zea mays* (maize) seedlings on agar also resulted in the development of LRs predominantly on the contact side of the root (Fig. 1 *E*, *F*, and *H* and *SI Appendix*, Fig. S3). In maize, LR development was also locally induced when seedlings were grown on wet germination paper, again indicating that no specific component of the medium besides water was necessary to elicit biased LR development (*SI Appendix*, Fig. S3). Using a similar experimental system as Karahara et al. (8) (Fig. 1*G*), we tested the effects of placing the maize primary root between two slabs of control media. Interestingly, LRs developed along both sides contacting the media, demonstrating that multiple distinct domains along the circumferential axis of the root can simultaneously form LRs with intervening areas lacking LR development (Fig. 1*H*).

X-ray microscale computed tomography (microCT) visualization of maize roots growing through a macropore (large air space) in the soil matrix revealed a similar positioning of LRs biased toward the root face in direct contact with the soil (Fig. 1*I*, Movie S1, and *SI Appendix*, Table S1). When roots were grown in pots without a macropore, LRs developed around the entire circumference of the primary root (Fig. 1*J* and Movie S2). Interestingly, when roots did not contact the soil surface in the macropore (Fig. 1*K* and Movie S3), LRs emerged sporadically in all directions, suggesting that a nonuniform environment is required for the bias in LR development but that contact is not required for LR development per se in this condition. These data support the physiological relevance of the patterning phenomenon observed in vitro.

In addition to LR emergence, rice and maize seedlings showed preferential accumulation of aerenchyma (air pockets forming in the cortex cell layers that may aid in gas exchange) on the air side of the root (Fig. 1 *E* and *F* and *SI Appendix*, Fig. S3). In maize, the pigment anthocyanin accumulated on the air side of the root whereas it was depleted from the contact side, especially in those regions where preemergent LRs were developing (*SI Appendix*, Fig. S3). This provided a useful visual marker to distinguish contact and air sides in root cross-sections. Anthocyanin biosynthesis is light-dependent; however, hydropatterning of LRs was not disrupted by growth of plants in the dark (*SI Appendix*, Fig. S3).

Rice, maize, and *Arabidopsis* also showed a clear bias in root hair development on the air side (Fig. 1 *E* and *F* and *SI Appendix*, Fig. S4). In *Arabidopsis*, suppression of root hair development often occurred before the initiation stage but was not associated with obvious changes in the expression of genes involved in root hair patterning (*SI Appendix*, Fig. S4). The presence of root hairs was used as a visual marker to distinguish air and contact sides of roots removed from the media for imaging. Root hair initiation on the contact side could be rescued by treatment with abscisic acid (ABA) or the ethylene precursor 1–aminocyclopropane-1–carboxylic acid (ACC), suggesting that the lack of root hair development was not simply a consequence of physical impedance

of the growth medium (*SI Appendix*, Fig. S4). Together these data demonstrated that plant roots are adept at sensing and developmentally responding to local differences in the environment in ways that we hypothesize take advantage of microscopic variations in the distribution of liquid water and air in soil.

The rate at which water is absorbed by the root (J_v) is the product of the driving force for water flow ($\Delta\Psi_w$, the difference in water potential between the root and the growth medium) and the resistance to water flow (inversely proportional to the hydraulic conductivities of the medium and the root, L_p) (9). In our in vitro growth systems, the air is likely at water-potential equilibrium with the culture medium; thus water potential does not distinguish these environments. Hydraulic conductivity, however, differs dramatically; the conductivity of agar (1×10^{-5} m^2 s^{-1} MPa^{-1}) is orders of magnitude higher than that of air (4.18×10^{-12} m^2 s^{-1} MPa^{-1}) (9, 10).

To specifically test the effects that media water potential and hydraulic conductivity have on the local regulation of LR development, we again used the "agar sandwich" approach to vary the media contacting the maize root (treatment agar slab) while a second agar slab contacting the root served as a control. In rice, Karahara et al. (8) previously showed that growth of roots between two slabs of agar results in asymmetries in aerenchyma development if one of the slabs contains mannitol, which reduces water potential of the medium. We performed similar experiments using polyethylene glycol (PEG; infused agar Ψ_w was -0.63 ± 0.02 MPa, and control agar was -0.10 ± 0.01 MPa) and observed a significant reduction in LR emergence on the treatment side, which partially mimicked the effect of air (Fig. 1*H*) (11). We severely reduced hydraulic conductivity by placing various non-water-conducting materials between the root and the treatment agar slab. This eliminated the inductive effect of this media on LR development, indicating that hydraulic conductivity of the contacted surface, rather than contact alone, was important for hydropatterning (*SI Appendix*, Fig. S3). Similar results were obtained when a sheet of glass or silicone rubber was used to contact the root, suggesting that the pliancy of the material was inconsequential (Fig. 1*H* and *SI Appendix*, Fig. S3). Together these data suggest that the rate with which water is absorbed by a root from the media determines whether a contacted surface will induce LR development.

To describe the environmental response phenomena shown here, we have designated the term hydropatterning: a nonuniform distribution of available water causes asymmetries in root development. This term is primarily used to simplify discussion of the process, and we do not intend to imply any specific physiological or molecular mechanisms used by the plant to detect differences in water availability.

Hydropatterning Affects Lateral Root Development During FC Specification. In *Arabidopsis*, the developmental steps involved in LR patterning have been well defined (12). Previous studies have clearly shown that environmental stimuli can affect the initiation and emergence of LRs (1); however, evidence is lacking regarding an earlier role. We predicted that if hydropatterning acts after LR initiation we should observe an accumulation of preemerged LR primordia on the air side, which would account for the lower relative number of emerged LRs on this side.

The *ProMiR390a:GFP-GUS* reporter is expressed in the xylem pole and associated pericycle cells and marks stage-I LR primordia and later stages (13) (Fig. 2*A*). Confocal imaging of contact and air sides of seedling primary roots showed a clear bias in the number of GFP-positive foci observed between these sides (Fig. 2*A*). The *ProDR5:VENUS-N7* reporter is initially expressed in adjacent xylem pole pericycle cells during FC activation and can be used to visualize the migration of nuclei from two neighboring pericycle cells to the common anticlinal cell plate before cell division and stage-I LR initiation (Fig. 2*B*) (14, 15). Interestingly, several stages of LR development showed a bias between the contact and air sides of the root, and no obvious accumulation of paused or quiescent LR primordia was observed on the air side that could account for the difference in emerged primordia between these sides (Fig. 2*B*). Quantification of LR primordia in seedlings after tissue clearing revealed similar results (*SI Appendix*, Fig. S5). These data indicate that hydropatterning acts at or before the earliest stages of LR initiation.

The orientation of the xylem pole determines the angle with which LRs emerge (5). Using the *ProS32:erGFP* reporter to mark the orientation of the vascular pole we found no significant bias with respect to the air–agar axis, eliminating this as a possible contributor to hydropatterning (*SI Appendix*, Fig. S5).

The earliest visual marker for the position of future LR primordia is the *ProDR5:LUC+* reporter, which marks PBSs. Moreno-Risueño et al. (4) previously showed that growth of roots on the surface or through agar had no significant influence on the number of PBSs specified, indicating that hydropatterning acts subsequent to PBS specification. Between the specification of PBSs along the longitudinal axis and the activation of asymmetric divisions in FCs, an additional decision must be made that has received less attention. In *Arabidopsis*, LRs will only develop from pericycle cells that overlie one of the two xylem poles (5). Although two such populations of cells exist along the circumferential axis of

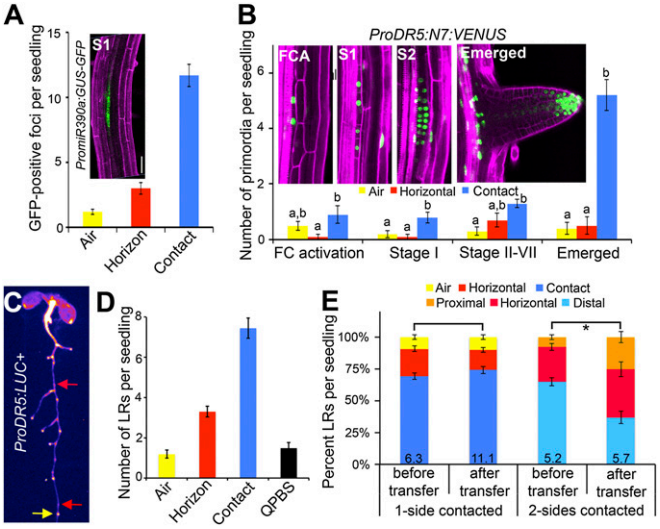

Fig. 2. Hydropatterning acts during FC specification to affect LR patterning. (*A*) The *PromiR390a:GUS-GFP* reporter is expressed at stage 1 of LR initiation and later. Confocal imaging of contact and air sides of the primary root showed a strong bias in the number of GFP-positive foci ($n \geq 10$). (*B*) The *ProDR5:N7:VENUS* reporter marks pericycle cell nuclei at the stage of FC activation (FCA), Stage 1 (S1), Stage 2 (S2), and later stages. Most stages showed greater numbers of primordia on the contact side than on the air side. (*C*) Seedling expressing the *ProDR5:LUC+* reporter. LR emergence patterns were quantified in the region of the primary root containing all emerged LRs (in this example, the region above the yellow arrow). Luciferase activity was then visualized, and foci of reporter activity, included outgrown LRs, were counted ($n = 27$). Quiescent PBSs (red arrows) are sites of reporter expression that showed no signs of LR emergence. (*D*) Chart showing the number of emerged LRs and quiescent PBSs (QPBS). (*E*) Seedlings were grown for 5 d on 1% agar, then a second agar slab was applied to the former air side of the root. Seedlings were grown for five additional days, and the position of emerged LRs was quantified in the region of the primary root that formed before and after treatment. Control seedlings were grown similarly; however, a second agar slab was not applied. The proximal domain is defined as the region of the primary root in contact with the second applied agar slab, whereas the distal domain is toward the original agar slab on which seedlings were germinated. In *B*, significant differences were analyzed on a per-stage basis using Student's *t* test ($P < 0.05$); statistically similar groups are indicated using the same letter. For *E*, asterisk indicates a significant difference based on Fisher's exact test ($P < 0.05$). Average number of LRs per centimeter of primary root shown at base of columns in bar charts. Error bars indicate SEM. (Scale bar, 50 μm.)

the root, pericycle cells adjacent to only one xylem pole are chosen. We postulated two models for how hydropatterning affects LR patterning during this developmental interval (*SI Appendix*, Fig. S6). In the first model, xylem pole selection and the subsequent specification of FCs at this pole are independent of the local environment, with the later stage of LR initiation being the target of hydropatterning. This model predicts that a similar number of FCs should be specified on the air and contact sides, with most FCs on the air side remaining quiescent. The second model postulates that local environmental differences across the circumferential axis bias xylem pole selection and FC specification toward the contact side. Based on this second model, we would expect few quiescent PBSs as most would be specified toward the permissive environment of the contacted surface to begin with.

Under our growth conditions, seedlings expressing the *ProDR5:LUC+* reporter developed on average 11.9 total emerged LRs after 10 d of growth with 7.4 LRs emerged toward the agar and 1.2 toward the air (Fig. 2 *C* and *D*). Thus, the difference in emerged LRs between air and contact sides is ∼6.3. To determine if there existed a quantity of quiescent PBSs that would account for this difference, we visualized the *ProDR5:LUC+* reporter and found 13.4 LUC-marked sites. We verified that reporter expression in PBSs was maintained throughout the time frame of the experiment (*SI Appendix*, Fig. S7). Based on the difference between the number of LUC-expressing foci and emerged LRs, we calculated that 1.5 PBSs were quiescent per seedling. This number is significantly lower than the number expected based on the first model (6.3 quiescent PBSs). Thus, our data are consistent with the second model and suggest that hydropatterning likely acts during FC specification.

If hydropatterning acts at FC specification, then mature regions of the primary root where FCs have already been specified should not be responsive to future changes in the distribution of water in the environment. By this reasoning, we predicted that regions of the root previously exposed to air would not develop new LRs if they subsequently came into contact with a wet surface. We directly tested this prediction by applying a sheet of agar to the air side of the root of an *Arabidopsis* seedling 5 d postgermination. The orientation of LR emergence was quantified in regions of the primary root that had formed before and after the application of the agar slab. In regions of the primary root previously exposed to air, the spatial distribution of LRs was similar in the treated roots to the untreated control, whereas in regions of the primary root that formed after application of the agar slab, LRs developed in all directions (Fig. 2*E*). These results are consistent with our model that hydropatterning acts at the time of FC specification and suggest that the orientation of LRs is determined through sensing of the local environment near the root tip and subsequently becomes fixed.

Auxin Biosynthesis Is Moisture-Induced and Necessary for Hydropatterning. We next asked which signaling pathways act downstream of moisture during hydropatterning. Previous work has shown that under water-limiting conditions, LR development is strongly suppressed (16). Severe water limitation induces ABA signaling, which is known to inhibit the development of LRs (17). We found that several mutants that disrupt ABA signaling did not have a significant effect on hydropatterning (*SI Appendix*, Fig. S8). Of particular importance, the *pyr/pyl 112458* mutant, which is highly resistant to ABA treatment (18), showed normal hydropatterning (*SI Appendix*, Fig. S8). These data differentiate hydropatterning from a classic water-stress response and indicate that signaling pathways other than ABA are involved.

Auxin is an important signaling molecule contributing to all stages of LR development (19). Quantification of indole-3–acetic acid (IAA) concentration in whole roots of *Arabidopsis* showed a significant increase when seedlings were grown on media with a lower concentration of agar (Fig. 3*A*). Measurements of endogenous auxin signaling using the *DII-VENUS* sensor, which is degraded in an auxin concentration-dependent manner (20), showed similar results (*SI Appendix*, Fig. S9). Furthermore, a transcriptional reporter of auxin response, *ProDR5:erGFP*, showed an increase in fluorescence in the outer tissue layers of the root at 1% agar compared with 3% agar conditions (*SI Appendix*, Fig. S9). These results suggest that water availability promotes auxin accumulation, signaling, and response.

We asked whether the auxin pathway was locally regulated by contact with a wet surface. Expression of the *DII-VENUS* sensor was lower on the contact side of the early maturation zone, relative to the air side, although no significant differences were observed elsewhere (Fig. 3 *B* and *C*). These data suggest that higher levels of auxin may be present on the contact side of the primary root. Determining differences in auxin signaling at the elongation zone and pericycle cell layers was not possible using

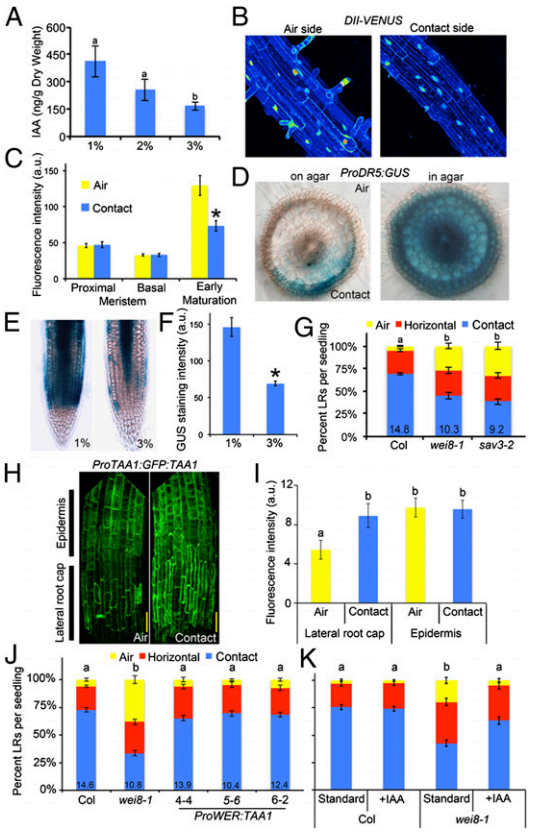

Fig. 3. Moisture activates auxin biosynthesis and response. (*A*) IAA levels quantified by liquid chromatography tandem mass spectrometry in whole roots grown on media containing different concentrations of agar ($n = 3$). (*B*) Maximum projects of confocal image stacks show *DII-VENUS* reporter expression is higher on the air side of the root relative to the contact side. Fluorescence intensity is shown using a 16-color look-up table. (*C*) Quantitation of *DII-VENUS* average nuclear fluorescence intensity in the epidermis shown for different regions of the root. (*D*) Cross-sections of rice roots expressing the *ProDR5:GUS* reporter showing local induction of the reporter on the contact side of the root (on agar) and uniform activation of the reporter when roots are grown in agar. (*E* and *F*) The *ProTIR2:TIR2:GUS* reporter shows stronger expression in the outer tissue layers of seedlings grown on 1% compared with 3% agar, quantified in *F*. (*G*) Two mutant alleles of tryptophan aminotransferase of *Arabidopsis* (*TAA1*) show a strong suppression of hydropatterning ($n \geq 20$). (*H*) Maximum projections of confocal image stacks show *ProTAA1:GFP:TAA1* reporter expression in the LRC and epidermis of the transition and elongation zones. (*I*) GFP fluorescence quantified for cell types on the air and contact sides ($n \geq 8$). (*J*) The *ProWER:TAA1* transgene was able to rescue the *wei8-1* hydropatterning defect in multiple independent transgenic lines as was growth of seedlings on media supplemented with IAA (*K*). Average number of LRs per seedling shown at base of columns in bar charts. Error bars indicate SEM. Significant differences based on Fisher's exact test ($P < 0.05$) (*G*, *J*, and *K*) or Student's *t* test ($P < 0.05$) (*A*, *C*, *F*, and *I*) with similar groups indicated using same letter. (Scale bars, 50 μm.)

the DII-VENUS sensor, as fluorescence intensity was very low in these regions of the root. In rice, where radial cross-sections are more easily examined, the auxin transcriptional response reporter, *ProDR5:GUS*, exhibited higher staining on the contact side of the early maturation zone compared with the air side, whereas uniform activation of the reporter was observed in roots grown through agar (Fig. 3*D*). Together these data suggest that water availability can locally promote auxin accumulation and its response.

TAA1 (also known as *WEI8*, *SAV3* and *TIR2*) encodes an L-tryptophan pyruvate aminotransferase that converts tryptophan to indole-pyruvic acid, a direct biosynthetic precursor of the auxin, IAA (21–26). The *ProTIR2:TIR2:GUS* reporter showed an increase in expression in the outer tissue layers at 1% agar compared with 3% agar media, suggesting *TAA1* may control water-dependent changes in auxin biosynthesis (Fig. 3 *E* and *F*). Indeed the *ProTAA1:TAA1:GFP* reporter line showed significant differences in expression level between the contact and air sides of the root (Fig. 3 *H* and *I*) for the lateral root cap (LRC); however, in the epidermis no differences were observed.

TAA1 loss-of-function alleles *wei8-1* and *sav3-1* both showed a significant reduction in hydropatterning (Fig. 3*G*), indicating that *TAA1*-mediated auxin biosynthesis is necessary for the response. To test if the spatial pattern of *TAA1* expression is important for hydropatterning, we attempted to rescue *wei8-1* defects by introducing transgenes that drove constitutive expression in the epidermis (*ProWEREWOLF:TAA1*) or throughout the root (*ProUBIQUTIN10:TAA1*). Both constructs were able to rescue hydropatterning in *wei8-1* and did not cause obvious gain-of-function defects (Fig. 3*J* and *SI Appendix*, Fig. S9). Furthermore, exogenous IAA added to the media could similarly rescue *wei8-1* defects (Fig. 3*K*). These data suggest that TAA1-mediated auxin biosynthesis is necessary for hydropatterning but that localized expression of TAA1 and local biosynthesis of IAA are not required to communicate positional information generated by the local environment.

Auxin Efflux and Response Pathways Are Necessary for Hydropatterning. Polar auxin transport is required to generate localized gradients of auxin important for patterning the site of future lateral organs (27). We treated seedlings with various concentrations of a transportable form of auxin, IAA, or 2,4-dichlorophenoxyacetic acid (2,4-D), which is not efficiently effluxed from cells (Fig. 4 *A* and *B*) (28). Although IAA did not have a significant effect, 2,4-D could strongly disrupt hydropatterning even at low concentrations, suggesting that the ability of the root to transport auxin may be important for hydropatterning. We surveyed various genetic backgrounds affected in PIN-mediated auxin efflux and found that the *Pro35S:PIN1* line strongly disrupted the process (*SI Appendix*, Fig. S10). Loss of pin-formed 3 (*PIN3*) function had a modest effect, which was enhanced in the *pin2/3/7* mutant background (Fig. 4*C*) (29). The *pin7* and the *pin3/7* double mutant also showed significant defects, whereas other *pin* alleles did not affect hydropatterning (*SI Appendix*, Fig. S10). These data indicate that a normal auxin transport pathway is required for hydropatterning, and this can be disrupted through misexpression of, or loss-of-function mutations in, certain transport pathway members.

We examined the spatial localization pattern of the PIN3 protein using a GFP reporter (*ProPIN3:PIN3:GFP*) and found specific enrichment in cortex and endodermal cells (ground tissue) overlying early-stage LR primordia on the contact side (Fig. 4 *D* and *E*). PIN3:GFP was localized to all surfaces of these cells and was particularly enriched at the cross-wall between neighboring cortex cells overlying LR primordia (Fig. 4*E*). Few early-stage primordia developed on the air side, and these were generally associated with very weak or absent PIN3:GFP expression. Quantification of these results revealed that early stage-I LR primordia were preferentially associated with these patches of PIN3:GFP expression on the contact side, and these primordia were able to progress through to later developmental stages (Fig. 4*F*). We did not observe ground tissue-associated PIN3 expression in the absence of a primordium, suggesting that PIN3 likely acts after FC specification and may promote

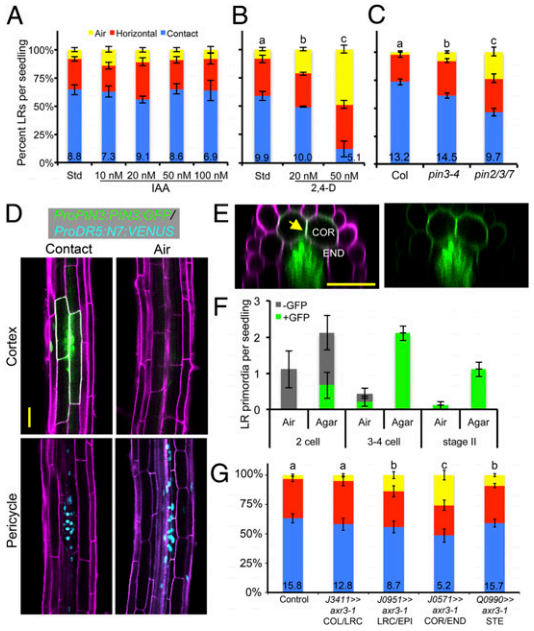

Fig. 4. Auxin efflux transport pathways are necessary for hydropatterning. Effect of IAA (*A*) or 2,4-D (*B*) treatment on hydropatterning ($n \geq 20$). (*C*) *pin3-4* and *pin2/3/7* mutants showed defects in hydropatterning ($n \geq 20$). (*D*) Roots expressing the *ProPIN3:PIN3:GFP* and *ProDR5:N7:VENUS* reporters. Optical cross-sections at the cortex cell layer (*Upper*) or at the pericycle (*Lower*). Propidium iodide counter stain (magenta), PIN3:GFP (green, plasma membrane localized), and N7:VENUS (cyan, nuclear). (*E*) A radial cross-section reveals strong localization to the lateral cross-walls between cortex cells (yellow arrow). (*F*) Frequency with which early stages of LR development are observed on the air and contact sides of the primary root and whether these primordia are associated with PIN3:GFP expression in ground tissue ($n = 9$). (*G*) Transactivation of *axr3-1* expression in the COR/END had the strongest effect in suppressing hydropatterning ($n \geq 20$). Average number of LRs per seedling shown at base of columns in bar charts. Error bars indicate SEM. Significant differences based on Fisher's exact test ($P < 0.05$) with similar groups indicated using same letter. (Scale bars, 50 μm.)

initiation of LR development on the contact side. This role for PIN3 is consistent with a previous study showing that PIN3 acts in the endodermis to promote LR initiation (30). Analysis of the PIN2 reporter did not reveal obvious differences in expression pattern between contact and air sides of the root (*SI Appendix*, Fig. S10). These data suggest that PIN transporters could play a role in maintaining local differences in auxin concentration between the air and contact sides but likely do not generate such gradients through differential expression or localization between these sides.

To probe where auxin transcriptional regulation is important for hydropatterning, we used the GAL4/UAS transactivation system to misexpress *axr3-1* in different cell layers (31). The *axr3-1* mutant allele encodes a dominant suppressor of auxin transcriptional responses (32). We observed significant reductions in hydropatterning in the *J0571>>axr3-1* line [cortex (COR) and endodermis (END)], and less in the *J0951>>axr3-1* [epidermis (EPI), weak cortex expression] and *Q0990>>axr3-1* [stele (STE), no pericycle (PER) expression] lines (Fig. 4*G*). Thus, ground tissue layers may be important conduits and response centers for auxin during hydropatterning. These data suggest that the perception of local moisture may occur through a cascade of signaling events initiated in the outer tissue layers that are transmitted ultimately to the pericycle.

Discussion

Through our studies of hydropatterning, we have revealed that the local distribution of water around the root tip plays an important role in the establishment of root system architecture

by biasing the position selected for future branch sites around the circumferential axis. Conservation of this process in eudicot and monocot species indicates that root systems of flowering plants have developed mechanisms to interpret and respond to microscale differences in the environment, which are relevant in natural soils. Hydropatterning also results in the biased development of other tissues such as aerenchyma and root hairs. Understanding the spatial scale at which stimuli are perceived and responses elicited is essential for predicting the impact that changes in the natural environment will have on plant physiology. Our studies of hydropatterning reveal that the regulation of LRs, hairs, and aerenchyma can result in distinct developmental zones over very small distances. Thus, perception, signaling, and response likely occur at the suborgan level. Signaling events controlling LR and root hair patterning occur at the root tip and become developmentally fixed. This has important implications for our understanding of root development under field conditions as we predict that periodic episodes of water deficit may have a long-term impact on root system architecture.

Our findings suggest that the availability of water from the environment, a product of hydraulic conductivity and water potential, is the critical environmental variable regulating LR development during hydropatterning. In the in vitro growth systems used here, differences in hydraulic conductivity are likely to be the major contributor to hydropatterning, as agar and air differ in this property by several orders of magnitude. We have also observed that hydropatterning is influenced by water potential; however, the effects are significant only with relatively large changes. If the water potential of the media is the same or lower than the water potential of the root itself, this would eliminate or reverse the flow of water from the media to the root and likely eliminate the LR-inducing effects of the media. How cells can actually sense differences in the availability of water from contacting surfaces will be an important and challenging question for future research.

Auxin biosynthesis, transport, and signaling are essential for hydropatterning. We have shown that differences in the availability of water affect the level of auxin that accumulates in the root and the expression level of *TAA1* in the outer tissue layers. Our data suggest that auxin levels may differ across the air-contact axis in *Arabidopsis* and rice roots and that specific PIN-type auxin efflux transporters may be important for maintaining gradients of auxin across the circumferential axis. Based on the spatial expression pattern of PIN transporters and mathematical-modeling approaches, it has been proposed that auxin is transported to the root tip through the central stele and then redirected away from the tip through the outer tissue layers (33, 34). We hypothesize that higher levels of auxin on the contact side are transported shootward through the outer tissues and delivered to the elongation and early maturation zones where they promote FC specification in pericycle cells at the proximal xylem pole. In the absence of *TAA1* or a properly functioning auxin transport pathway, auxin signaling may not reliably exceed the required threshold on the contact side to influence the spatial distribution of FCs. Root curvature is proposed to act after FC specification (4), thus explaining why we do not observe an interaction with hydropatterning.

Materials and Methods

Plant materials and methods for genetic analysis, plant growth conditions, transgene construction, phenotypic analysis, and X-ray microscale computed tomography (microCT) are described in *SI Appendix, SI Materials and Methods*. *Arabidopsis thaliana* ecotypes Columbia, Col-0, and Landsberg *erecta* [La(*er*)] were used. Maize inbred line B73 and rice cultivar Kitaake and Taichung 65 were used.

ACKNOWLEDGMENTS. We thank José Alonso, Fred Berger, Eva Benkova, Matt Evans, Annemarie Meijer, Ben Scheres, and Jian Xu for providing materials, and the J.R.D. laboratory for comments on the manuscript. Funding was provided by a Carnegie Institution for Science endowment, the National Research Foundation of Singapore, a National Science Foundation Graduate Research Fellowship under Grant DGE-1147470 (to N.E.R.), European Research Council FUTUREROOTS (C.J.S., M.C.T., S.J.M., and M.J.B.), and Biotechnology and Biological Sciences Research Council (C.J.S., S.J.M., and M.J.B.).

1. Malamy JE (2005) Intrinsic and environmental response pathways that regulate root system architecture. *Plant Cell Environ* 28(1):67–77.
2. Overvoorde P, Fukaki H, Beeckman T (2010) Auxin control of root development. *Cold Spring Harb Perspect Biol* 2(6):a001537.
3. De Smet I, et al. (2007) Auxin-dependent regulation of lateral root positioning in the basal meristem of Arabidopsis. *Development* 134(4):681–690.
4. Moreno-Risueño MA, et al. (2010) Oscillating gene expression determines competence for periodic Arabidopsis root branching. *Science* 329(5997):1306–1311.
5. Parizot B, et al. (2008) Diarch symmetry of the vascular bundle in Arabidopsis root encompasses the pericycle and is reflected in distich lateral root initiation. *Plant Physiol* 146(1):140–148.
6. Brady NC, Weil RR (2008) *The Nature and Properties of Soils* (Pearson–Prentice Hall, Upper Saddle River, NJ), Revised 14th Ed.
7. Owens L, Wozniak C (1991) Measurement and effects of gel matric potential and expressibility on production of morphogenic callus by cultured sugarbeet leaf discs. *Plant Cell Tissue Organ Cult* 26(2):127–133.
8. Karahara I, et al. (2012) Demonstration of osmotically dependent promotion of aerenchyma formation at different levels in the primary roots of rice using a 'sandwich' method and X-ray computed tomography. *Ann Bot (Lond)* 110(2):503–509.
9. Nobel PS, Cui M (1992) Shrinkage of attached roots of *Opuntia ficus-indica* in response to lowered water potentials—Predicted consequences for water uptake or loss to soil. *Ann Bot (Lond)* 70(6):485–491.
10. Ishida T, Anno T, Matsukawa S, Nagano T (2000) Hydraulic conductivity and diffusion coefficient in gels for plant tissue culture. *Environ Control Biol* 38(3):165–171.
11. Verslues PE, Agarwal M, Katiyar-Agarwal S, Zhu J, Zhu JK (2006) Methods and concepts in quantifying resistance to drought, salt and freezing, abiotic stresses that affect plant water status. *Plant J* 45(4):523–539.
12. Van Norman JM, Xuan W, Beeckman T, Benfey PN (2013) To branch or not to branch: The role of pre-patterning in lateral root formation. *Development* 140(21):4301–4310.
13. Marin E, et al. (2010) miR390, Arabidopsis TAS3 tasiRNAs, and their AUXIN RESPONSE FACTOR targets define an autoregulatory network quantitatively regulating lateral root growth. *Plant Cell* 22(4):1104–1117.
14. Laskowski M, et al. (2008) Root system architecture from coupling cell shape to auxin transport. *PLoS Biol* 6(12):e307.
15. De Rybel B, et al. (2010) A novel aux/IAA28 signaling cascade activates GATA23-dependent specification of lateral root founder cell identity. *Curr Biol* 20(19):1697–1706.
16. Babé A, et al. (2012) Repression of early lateral root initiation events by transient water deficit in barley and maize. *Philos Trans R Soc Lond B Biol Sci* 367(1595):1534–1541.
17. De Smet I, et al. (2003) An abscisic acid-sensitive checkpoint in lateral root development of Arabidopsis. *Plant J* 33(3):543–555.
18. Gonzalez-Guzman M, et al. (2012) Arabidopsis PYR/PYL/RCAR receptors play a major role in quantitative regulation of stomatal aperture and transcriptional response to abscisic acid. *Plant Cell* 24(6):2483–2496.
19. Lavenus J, et al. (2013) Lateral root development in Arabidopsis: Fifty shades of auxin. *Trends Plant Sci* 18(8):450–458.
20. Brunoud G, et al. (2012) A novel sensor to map auxin response and distribution at high spatio-temporal resolution. *Nature* 482(7383):103–106.
21. Stepanova AN, et al. (2011) The Arabidopsis YUCCA1 flavin monooxygenase functions in the indole-3-pyruvic acid branch of auxin biosynthesis. *Plant Cell* 23(11):3961–3973.
22. Stepanova AN, et al. (2008) TAA1-mediated auxin biosynthesis is essential for hormone crosstalk and plant development. *Cell* 133(1):177–191.
23. Yamada M, Greenham K, Prigge MJ, Jensen PJ, Estelle M (2009) The TRANSPORT INHIBITOR RESPONSE2 gene is required for auxin synthesis and diverse aspects of plant development. *Plant Physiol* 151(1):168–179.
24. Tao Y, et al. (2008) Rapid synthesis of auxin via a new tryptophan-dependent pathway is required for shade avoidance in plants. *Cell* 133(1):164–176.
25. Won C, et al. (2011) Conversion of tryptophan to indole-3-acetic acid by TRYPTOPHAN AMINOTRANSFERASES OF ARABIDOPSIS and YUCCAs in Arabidopsis. *Proc Natl Acad Sci USA* 108(45):18518–18523.
26. Mashiguchi K, et al. (2011) The main auxin biosynthesis pathway in Arabidopsis. *Proc Natl Acad Sci USA* 108(45):18512–18517.
27. Benková E, et al. (2003) Local, efflux-dependent auxin gradients as a common module for plant organ formation. *Cell* 115(5):591–602.
28. Delbarre A, Muller P, Imhoff V, Guern J (1996) Comparison of mechanisms controlling uptake and accumulation of 2,4-dichlorophenoxy acetic acid, naphthalene-1-acetic acid, and indole-3-acetic acid in suspension-cultured tobacco cells. *Planta* 198(4):532–541.
29. Blilou I, et al. (2005) The PIN auxin efflux facilitator network controls growth and patterning in Arabidopsis roots. *Nature* 433(7021):39–44.
30. Marhavý P, et al. (2013) Auxin reflux between the endodermis and pericycle promotes lateral root initiation. *EMBO J* 32(1):149–158.
31. Swarup R, et al. (2005) Root gravitropism requires lateral root cap and epidermal cells for transport and response to a mobile auxin signal. *Nat Cell Biol* 7(11):1057–1065.
32. Rouse D, Mackay P, Stirnberg P, Estelle M, Leyser O (1998) Changes in auxin response from mutations in an AUX/IAA gene. *Science* 279(5355):1371–1373.
33. Grieneisen VA, Xu J, Marée AF, Hogeweg P, Scheres B (2007) Auxin transport is sufficient to generate a maximum and gradient guiding root growth. *Nature* 449(7165):1008–1013.
34. Band LR, et al. (2014) Systems analysis of auxin transport in the Arabidopsis root apex. *Plant Cell* 26(3):862–875.

Supplementary Information

SI Materials and Methods

Plant materials

Mutants, *abi1-1* (1), and *abi2-1* (2) are in the *La(er)* background. The *wei8-1* (3), *sav3-2* (4), *pyr/pyl112458* sextuple mutant (5), *nced2*, *nced5*, *nced9* (6), *pin3-4 (SALK_005544)*, and *pin2/3/7* (7) mutations and the *ProCOBL9:GFP-GUS* (8), *ProGL2:erGFP* (9), *ProWER:erGFP* (10), *Pro35S:PIN1* (11), *ProUAS:axr3-1* (12), *ProDR5:LUC+* (13), *ProPIN3:PIN3:GFP* (14), *DII:VENUS* (15), *PromiR390a:GUS:GFP* (16), *ProDR5:erGFP* (17), *ProDR5:erGFP* in *wei8* and *ProTAA1:GFP:TAA1* (3), *ProS32:erGFP* (17) transgenes are in the *Col-0* background. *GAL4-VP16/UAS* enhancer trap lines *J3411*, *J0951*, *J2812*, *J0571*, *Q2500*, *Q0990*, *J0121* are in the *C24* background (18). Rice cultivar Kitaake was used for quantification of LR and aerenchyma development. The *ProDR5:GUS* reporter line in *Oryza sativa* (L.) Japonica cultivar Taichung 65 was previously described (19).

Genetic analysis

To selectively express *axr3-1* in specific tissue layers of the root, different enhancer trap lines were crossed to plants harboring the *UAS:axr3-1* transgene. Wild-type plants of the C24 ecotype were crossed with *UAS:axr3-1* plants to generate the control genotype. Phenotypic and gene expression analyses were performed using the F1 progeny.

Plant growth conditions

Arabidopsis seeds were surface sterilized and seedlings grown as previously described (18). Standard media is as described (18). Seedlings were grown for 10 days before the emergence patterns of lateral roots were quantified. The effect of various hormones was determined in seedlings first grown for 5 days on standard media then transfered to standard media or media supplemented with various chemicals for 5 days before phenotyping. The position of the root tip was marked at the time of transfer and LR development characterized only in the region that developed after transfer. Supplements include abscisic acid (ABA, Sigma-Aldrich), 2,4-dichlorophenoxyacetic acid (2,4-D, Sigma-Aldrich) and indole-3-acetic acid (IAA, Sigma-Aldrich). In some experiments, 2% or 3% w/v agar was added to the media or Gelrite (Gellan Gum, Sigma-Aldrich) was used in place of agar.

Rice seeds were sterilized using 70% EtOH for 2 minutes followed by a 50% bleach solution for 5 minutes and rinsed twice with sterile water. Seeds were dried on filter paper and germinated on MS agar media at 28°C.

Maize kernels were soaked for 4 hours in deionized water at room temperature, and tip caps were removed. Kernels were then incubated in a 55-57°C water bath for 5 minutes followed by incubation in a 20% bleach/0.1% Tween-20 solution for 20 minutes. Kernels were washed 5-7 times with sterile deionized water and plated immediately. Seedlings were grown on sterile 1% agar media containing 1/2X MS nutrients and 0.5 g/L MES, adjusted to pH 5.7 with KOH. Tissue culture plates were tilted 60° from the horizontal axis until root tips contacted the surface of the medium, after which point the plates were positioned vertically.

For the MicroCT assessment of LR formation in soil, a Newport series loamy sand (sand 83.2%, silt 4.7%, and clay 12.1%; pH 6.35; organic matter 2.93%; FAO Brown Soil) taken from the University of Nottingham farm at Bunny, Nottinghamshire, UK (52.8586°, -1.1280°) was packed into a plastic soil column (30 mm diameter x 100 mm length) to a typical field bulk density of 1.1 g cm^{-1}. Eight replicate columns were saturated with water from the bottom and then allowed to freely drain for two days to notional field capacity. To compare LR formation between soil cores with or without a macropore (to give a scenario where the root has only partial contact with a moist soil surface), a vertical macropore was created in the center of each core using a 7 mm diameter core borer for half of the replicates. A pre-germinated maize kernel was positioned at either the center (no macropore samples) or the top edge of the macropore and then covered with moist soil taking care not to fill the macropore with soil. Plants were subsequently grown for 5 days at 25°C before X-ray microCT scanning. The water content of the soil at field capacity was moist (approximately 26 % moisture), therefore, it was expected the air within the macropore would have a humid microclimate.

Transgene construction

The primers 5'-GGG GAC AAC TTT GTA TAG AAA AGT TGg ggc cca ata ctg acc taa gat ttt gc-3' and 5'-GGG GAC TGC TTT TTT GTA CAA ACT TGt ctt ttt gtt tct ttg aat gat ag-3' were used to clone a 2.5 kb fragment of the *WEREWOLF* (AT5G14750) promoter and 5'-GGG GAC AGC TTT CTT GTA CAA ATG TGT Ttg tgt ttt ctg ctt ttg tta ttt tag-3' and 5'-GGG GAC AAC TTT GTA TAA TAA AGT TGT gat atc gtt ttg ctg aag ttg ctt t-3' were used to clone a 1 kb fragment of the *WEREWOLF* 3'UTR into pDONRP4-P1R and pDONRP2R-P3 Gateway vectors, respectively. The primers 5'-CAC CAT GGT GAA ACT GGA GAA CTC GA-3' and 5'-CTA AAG GTC AAT GCT TTT AAT GAG CT3' were used to PCR amplify the *TAA1* (AT1G70560) coding sequence from cDNA synthesized using *Col-0* root RNA and cloned into the D-TOPO vector. Multisite Gateway (Invitrogen) recombination was used to introduce the *ProWER:TAA1, ProUAS:TAA1* and *ProUBQ10:TAA1* minigenes into the pCherry-pickerT destination vector, which contains a *Pro35S:PM-mCherry* selection marker gene (18). The Agrobacterium strain GV3101 transformed with the *pSoup* vector, was used for plant transformation as previously described (18).

Phenotypic Analysis

The direction of LR emergence was characterized in *Arabidopsis* seedlings grown on standard media for 10 days before observation. LRs were visualized using a dissecting microscope (Olympus SZ61) and categorized into 3 different phenotypic groups (air side, horizon side and contact side) based on the initial direction of emergence from the primary root relative to the media surface. LRs emerging on the contact side were categorized as such if the emergence site of the LR from the epidermis was below the horizon of the root and could not be seen by viewing from above. LRs emerging on the horizon side were characterized as such if the emergence site could be seen and the angle of LR growth was parallel to the agar surface. LRs emerging on the air side were characterized as such if the emergence site could be observed and the LR was initially growing towards the observer. To ensure consistency in the results, two researchers independently conducted initial phenotypic analysis of mutants. For confocal imaging of

contact and air sides, the presence of root hairs was used as a visual marker for the air side of the root while lack of hairs marked the contact side. The *ProTAA1:GFP:TAA1* reporter line lacks root hairs. To visualize differences in GFP intensity between contact and air sides for this reporter, roots were rotated 90° then imaged the next day. The 90° bend allowed the roots to positioned on the glass slide so that air or contact sides were facing the cover slip.

For "agar sandwich" experiments using maize seedlings, sandwiches were assembled as depicted in (Fig. 1G) and based on previous designs (20). Seeds were sterilized then imbibed on sterile germination paper at 29°C for three days. Seedlings were then transferred to 2% (w/v) agar media, primary roots were flanked with 1/32"-thick silicone rubber spacers (McMaster-Carr, 86045K31) and Treatment agar blocks were placed against the exposed side of the roots. Zap-A-Gap CA+ super glue (Super Glue Corporation) was used to affix the silicone rubber to the Control and Treatment agar blocks. Blot paper (Whatman) was placed between the root and either agar block to prevent the primary root tip from penetrating into the agar. Treatment agar media was infused with a PEG-8000 (Sigma-Aldrich) solution or mock-infused with liquid growth medium (21). For the Parafilm/Agar, Plastic Wrap/Agar, and Silicone/Agar treatments (Fig. S3), the sheet of blot paper on the Treatment block was replaced with the corresponding material, which was affixed to the block using super glue. For the Air/Control treatment (Fig. 1K), no Treatment agar block was applied to the root. For the Glass/Agar treatment (Fig. S2), a microscope slide was used in place of the Treatment agar block. Positions of root tips at the time of sandwich assembly were marked on the plate. Seedlings were grown in sandwiches for 5 days, and LRs were quantified from the transfer point to the physical end of the treatment agar block. Water potential measurements for solid agar media were made using a Wescor Vapor Pressure Osmometer 5500 at the time of sandwich assembly and at the end of the experiment to ensure that differences in water potential were maintained throughout the experiment. Water potential measurements were made in triplicate for each sample and averaged.

Treatment of Arabidopsis seedlings with an agar slab was performed on 5 dpg seedlings. A sheet of control media was excised and placed on top of the seedling root and affixed using super glue. The position of the root tip was marked and seedlings were allowed to grow under standard conditions for 5 additional days before the orientation of LRs were quantified in the two regions of the root.

The Fisher's exact test was used to determine statistical significance for differences in LR distribution between genotypes or treatments using a P-value threshold of < 0.05. Air, horizon and contact were considered three categories and the number of LRs quantified from the seedlings analyzed were pooled together for the test.

Glucuronidase (GUS) reporter assays and sample preparation were performed as previously described (18). For confocal microscopy, roots were mounted in a propidium iodide solution (5 µg/ml) (Invitrogen), and imaged using a Leica SP5 point-scanning confocal microscope or a Leica DM6000 inverted microscope equipped with a Yokogawa CSU-X spinning disk confocal head and a Roper Evolve camera. The imaging settings were 488 nm excitation and 505-550 nm emission for GFP, 514 nm excitation and 520-560 nm emission for YFP or VENUS and 488 nm excitation and >585 nm emission for propidium iodide. Quantification of relative fluorescence intensity was performed using Fiji (22).

For luminescence imaging, *ProDR5:LUC+* seedlings were sprayed with a 2 mM sodium D-luciferin (Gold Biotechnology) solution and imaged using a customized luminescence imaging system. Images of seedlings were taken in the following sequence: one bright-field image with external illumination followed by a 5 minute dark interval then a 3-5 minute exposure with no illumination. The expression of *ProDR5:LUC+* was characterized in the region between the first and the last visible emerged LR. The number of PBSs (*LUC* expressing foci) was counted within this region including emerged LR.

Levels of IAA in plant tissue were quantified as previously described (22).

X-ray microscale Computed Tomography (microCT)

All CT scanning was performed using a Phoenix Nanotom 180NF (GE Sensing & Inspection Technologies GmbH, Wunstorf, Germany) at a maximum electron acceleration energy of 110 kV, 110 µA current and acquiring a total of 1,440 projection images over a 360° rotation. Each projection image was the average of 3 images acquired with a detector exposure time of 500 msec. The resulting isotropic voxel edge length was 22 µm and the total scan time was 60 minutes. The dose to the center of each macrocosm was calculated at 4.5 Gy (23). Reconstruction of the projection images to produce 16 bit, 3-D volumetric data sets was performed using the software datos|rec (GE Sensing & Inspection Technologies GmbH, Wunstorf, Germany). Image sections and 3D rendered images was performed using VG StudioMax Version 2.2 (Volume Graphics GmbH, Heidelberg, Germany). LRs were visually scored from the images based on their emergence at either the root/air or root/soil boundary.

References

1. Koornneef M, Reuling G, & Karssen CM (1984) The isolation and characterization of abscisic acid-insensitive mutants of *Arabidopsis thaliana*. *Physiol. Plant.* 61:377-383.
2. Leung J, Merlot S, & Giraudat J (1997) The Arabidopsis ABSCISIC ACID-INSENSITIVE2 (ABI2) and ABI1 genes encode homologous protein phosphatases 2C involved in abscisic acid signal transduction. *Plant Cell* 9(5):759-771.
3. Stepanova AN*, et al.* (2008) TAA1-mediated auxin biosynthesis is essential for hormone crosstalk and plant development. *Cell* 133(1):177-191.
4. Tao Y*, et al.* (2008) Rapid synthesis of auxin via a new tryptophan-dependent pathway is required for shade avoidance in plants. *Cell* 133(1):164-176.
5. Antoni R*, et al.* (2013) PYRABACTIN RESISTANCE1-LIKE8 plays an important role for the regulation of abscisic acid signaling in root. *Plant Physiol.* 161(2):931-941.
6. Toh S*, et al.* (2008) High temperature-induced abscisic acid biosynthesis and its role in the inhibition of gibberellin action in Arabidopsis seeds. *Plant Physiol.* 146(3):1368-1385.
7. Blilou I*, et al.* (2005) The PIN auxin efflux facilitator network controls growth and patterning in Arabidopsis roots. *Nature* 433(7021):39-44.

8. Brady SM, Song S, Dhugga KS, Rafalski JA, & Benfey PN (2007) Combining expression and comparative evolutionary analysis. The COBRA gene family. *Plant Physiol.* 143(1):172-187.
9. Lin Y & Schiefelbein J (2001) Embryonic control of epidermal cell patterning in the root and hypocotyl of *Arabidopsis*. *Development* 128(19):3697-3705.
10. Lee MM & Schiefelbein J (1999) WEREWOLF, a MYB-related protein in Arabidopsis, is a position-dependent regulator of epidermal cell patterning. *Cell* 99(5):473-483.
11. Benková E*, et al.* (2003) Local, efflux-dependent auxin gradients as a common module for plant organ formation. *Cell* 115(5):591-602.
12. Swarup R*, et al.* (2005) Root gravitropism requires lateral root cap and epidermal cells for transport and response to a mobile auxin signal. *Nature Cell Bio.* 7(11):1057-1065.
13. Moreno-Risueño MA*, et al.* (2010) Oscillating gene expression determines competence for periodic Arabidopsis root branching. *Science* 329(5997):1306-1311.
14. Zadnikova P*, et al.* (2010) Role of PIN-mediated auxin efflux in apical hook development of Arabidopsis thaliana. *Development* 137(4):607-617.
15. Brunoud G*, et al.* (2012) A novel sensor to map auxin response and distribution at high spatio-temporal resolution. *Nature* 482(7383):103-106.
16. Marin E*, et al.* (2010) miR390, Arabidopsis TAS3 tasiRNAs, and their AUXIN RESPONSE FACTOR targets define an autoregulatory network quantitatively regulating lateral root growth. *Plant Cell* 22(4):1104-1117.
17. Lee JY*, et al.* (2006) Transcriptional and posttranscriptional regulation of transcription factor expression in Arabidopsis roots. *Proc. Natl. Acad. Sci. USA* 103(15):6055-6060.
18. Duan L*, et al.* (2013) Endodermal ABA signaling promotes lateral root quiescence during salt stress in Arabidopsis seedlings. *Plant Cell* 25(1):324-341.
19. Scarpella E, Rueb S, & Meijer AH (2003) The RADICLELESS1 gene is required for vascular pattern formation in rice. *Development* 130(4):645-658.
20. Karahara I*, et al.* (2012) Demonstration of osmotically dependent promotion of aerenchyma formation at different levels in the primary roots of rice using a 'sandwich' method and X-ray computed tomography. *Ann. Bot. (Lond)* 110(2):503-509.
21. Verslues PE, Agarwal M, Katiyar-Agarwal S, Zhu J, & Zhu JK (2006) Methods and concepts in quantifying resistance to drought, salt and freezing, abiotic stresses that affect plant water status. *Plant J.* 45(4):523-539.
22. Geng Y*, et al.* (2013) A spatio-temporal understanding of growth regulation during the salt stress response in Arabidopsis. *Plant Cell 25(6):2132-54*.
23. Mairhofer S*, et al.* (2013) Recovering complete plant root system architectures from soil via X-ray mu-Computed Tomography. *Plant Methods* 9(1):8.
24. Fukaki H & Tasaka M (2009) Hormone interactions during lateral root formation. *Plant Mol. Biol.* 69(4):437-449.

Table S1. Quantitation of LR development in microCT imaging trials.

Soil Column ID	Pore	Total lateral roots	Lateral roots emerging in air	Comments
2	No	79	0	
3	No	77	0	
11	No	67	0	
12	No	61	0	
13	Yes	14	14	Primary Root not in contact with soil
14	Yes	39	6	
15	Yes	24	0	All roots grew into soil
B73-1	Yes	8	0	All roots grew into soil
B73-2	Yes	0	0	
B73-3	Yes	0	0	

Fig. S1

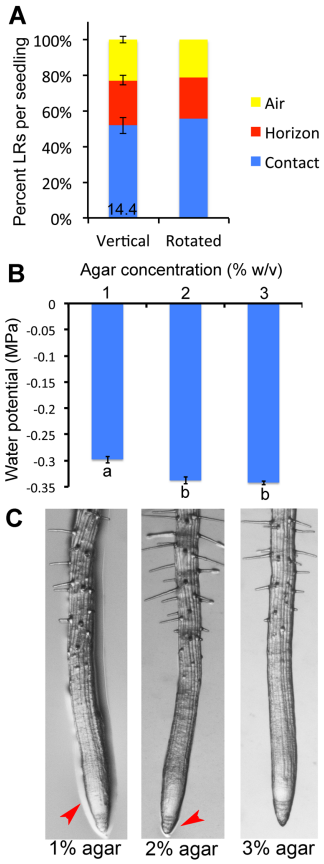

Fig. S1. Root bending does not affect hydropatterning; agar concentration affects water potential and the size of the meniscus that contacts the root.
(A) Effect of root bending on hydropatterning. Seedlings were grown vertically (n=22) or gravitationally stimulated (n=52) by rotating 90°. The direction LRs emerged around the circumferential axis (hydropatterning) was quantified over the entire length of the primary root for vertically grown seedlings. For rotated seedlings, LR emergence was quantified for a single LR that was induced nearest to the most convex region of the bend. (B) Water-potential measurements of media containing different concentrations of agar. (C) Primary roots grown on different media. Red arrowheads mark the meniscus. Error bars indicate SEM. Significant differences based on Student's T-test ($P < 0.05$) and similar groups indicated using same letter.

Fig. S2

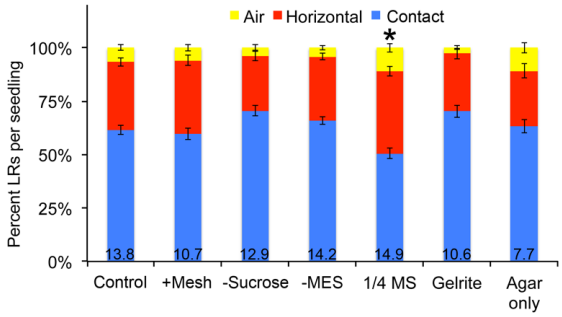

Fig. S2. Components used in the growth media are not necessary for hydropatterning. To test which, if any, components of the media used influenced hydropatterning, we characterized LR emergence in seedlings germinated on various media: Control, standard media with 1% sucrose, 1X MS, 0.5 g/l MES and 1% agar (Ψ_w = -0.29 MPa), +Mesh, standard media with overlying nylon mesh separating the root from the agar surface, -Sucrose, standard media without sucrose (Ψ_w = -0.22 MPa), -MES, standard media without MES (Ψ_w = -0.33 MPa), ¼ MS, standard media with 1/4X MS (Ψ_w = -0.23 MPa), Gelrite, standard media with gelan gum instead of agar (Ψ_w = -0.36 MPa), Agar only, no other component of standard media except agar (Ψ_w = -0.14 MPa) ($n > 20$). Average number of LRs per seedling shown at base of columns in bar charts. Error bars indicate SEM. Asterisk marks significant difference based on Fisher's exact test, P-value < 0.05, however after multiple testing correction (Bonferroni) the difference is not significant.

Fig. S3.

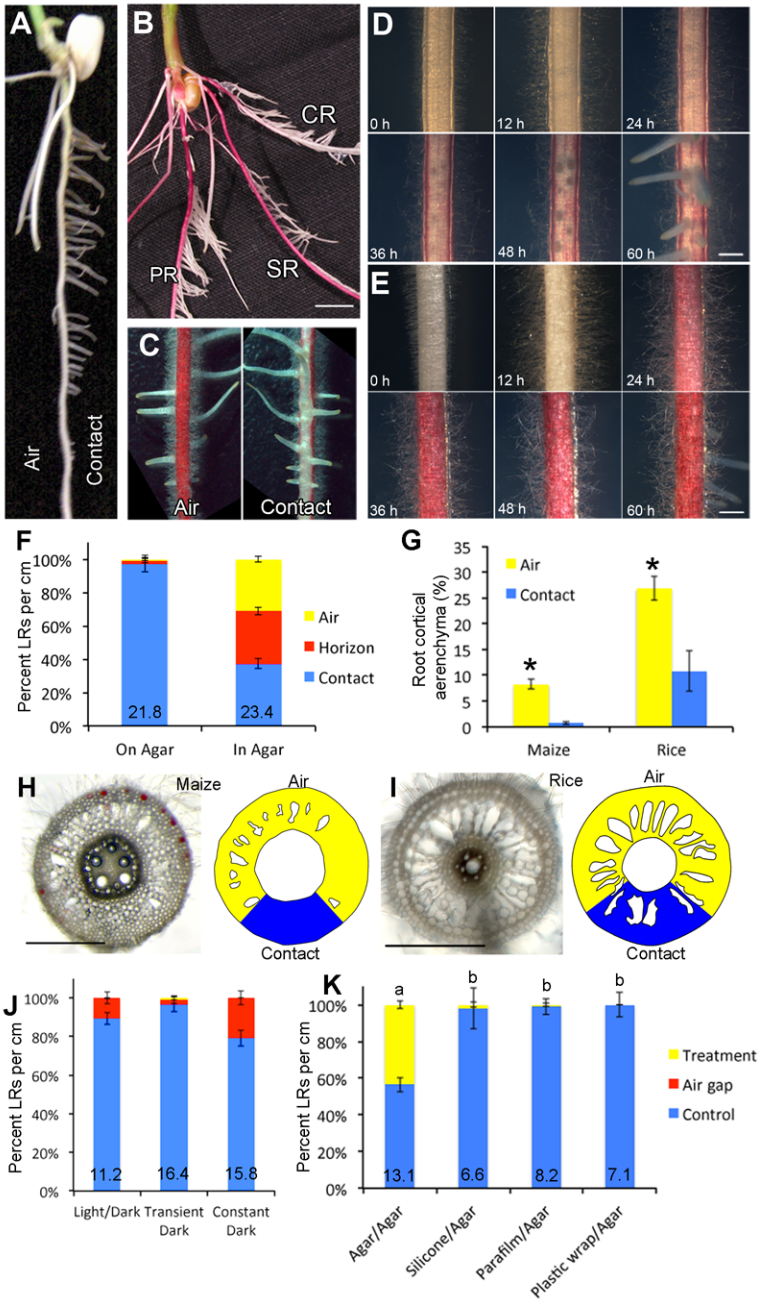

Fig. S3. Grass roots exhibit hydropatterning of LR and aerenchyma development and anthocyanin.

(A) A rice seedling grown on agar showing LRs only on the contact side of the primary root. (B) A maize seedling grown on agar and removed from media for image capture. Primary root (PR), seminal root (SR) grown on agar and showing hydropatterning and crown root (CR) grown through agar showing a reduction in anthocynanin accumulation and no hydropatterning. (C) Hydropatterning of the maize primary root grown on germination paper with water. (D) Time-lapse images of the contact side of a maize primary root showing the development of LRs. Pre-emergent LRs can be identified by

the local suppression of anthocyanin accumulation in the overlying tissues. (E) On the air side of the root, hair development and anthocyanin accumulation are apparent. (F) Bias in the orientation of emerged LRs in rice primary roots grown on the surface of an agar medium or in the agar ($n \geq 9$). (G) Percentage of cortical tissue area that is aerenchyma in maize (20 cross-sections from 4 roots quantified) and rice (11 cross-sections from 3 roots quantified). Cortex aerenchyma on the contact and air sides quantified separately. (H, I) Brightfield images of maize and rice root cross-sections (left) and diagram showing air (yellow) and contact (blue) regions and aerenchyma (outlined spaces) as quantified in (G). (J) Hydropatterning in maize roots grown under standard long day light conditions (light/dark), for a 24-hour period of darkness (transient dark) or in complete darkness throughout growth (constant dark) ($n \geq 8$). (K) The "agar sandwich" approach was used to test the effect of various pliant surfaces that have low water conductivities on LR development ($n=4$ seedlings per conditions). LR outgrowth is induced on two sides by contact with agar (Agar/Agar); this effect is lost when silicone rubber is used in place of one of the agar slabs (Silicone/Agar) or if the agar is covered by parafilm (Parafilm/Agar) or plastic wrap (Plastic wrap/Agar). Average number of LRs per seedling shown at base of columns in bar charts. Error bars indicate SEM. Significant differences based on Fisher's exact test ($P < 0.05$) with similar groups indicated using same letter (K) or Student's T-test ($P < 0.05$) with significant differences labeled with asterisk (G). Scale Bar is 1 mm (B, D, E), 0.5 mm (H) and 0.25 mm (I).

Fig. S4

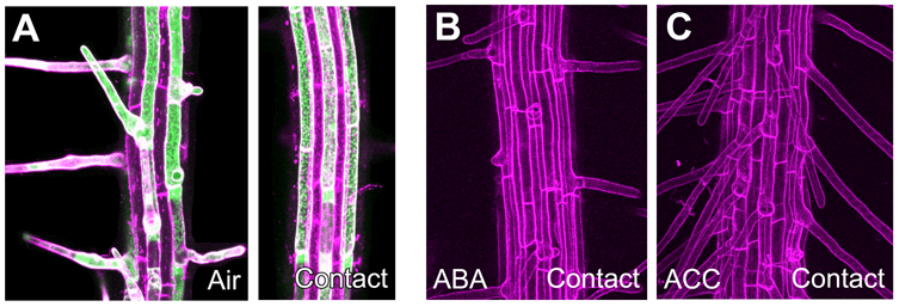

D

	Trichoblast lineage		Atrichoblast lineage	
	root hairs initiated	cell counted	root hairs initiated	cell counted
Col-0 Air side	86	86	0	78
Col-0 Contact side	1	51	0	38

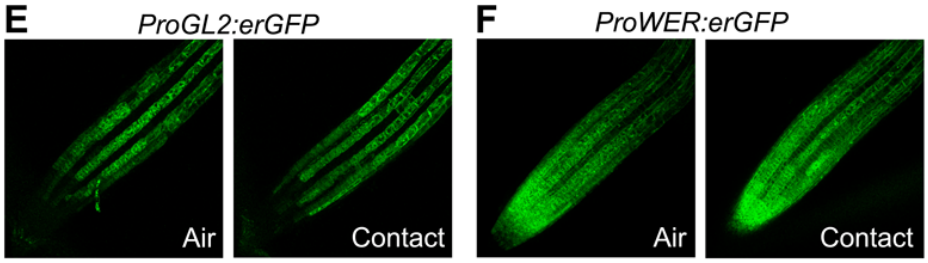

Fig. S4. Hydropatterning of root hair initiation in Arabidopsis roots.
(A) The *ProCOBL9:GFP-GUS* reporter marks trichoblast-lineage cells and is expressed in a similar pattern on the air and contact sides while hairs are only observed on the air side. (B, C) Addition of 5 μM ACC or 10 μM ABA rescues root hair initiation. (D) The number of root hairs that develop per epidermal cell was quantified for cells in the trichoblast lineage (H-position) and atrichoblast lineage (N-position) based on whether they were overlying cortex cells or cortex cell T-junctions. Note that few contact-side trichoblast lineage cells initiate a root hair. (E, F) The atrichoblast cell markers *ProGL2:erGFP* and *ProWER:erGFP* do not show obvious differences in expression pattern between the air and contact sides of the root.

Fig. S5.

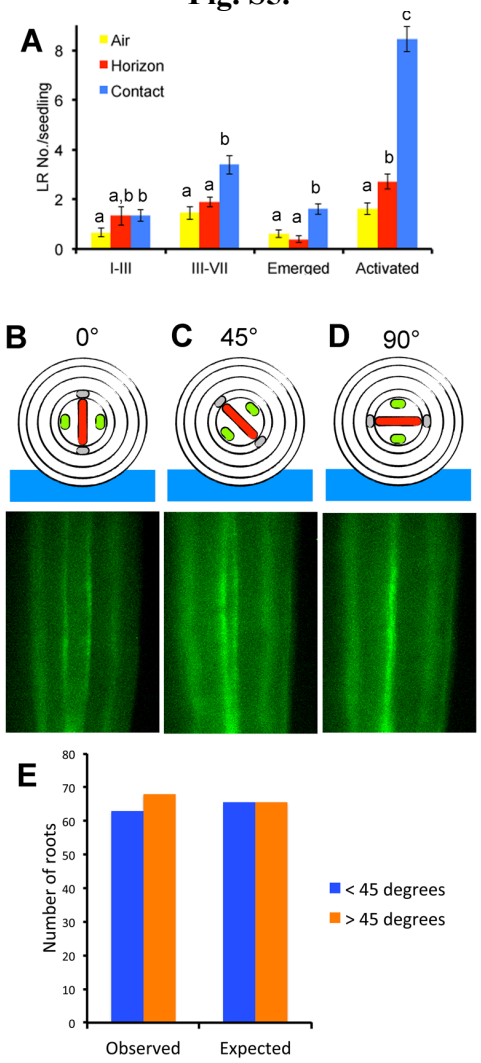

Fig. S5 Hydropatterning of pre-emergent LRs; vascular orientation is not biased by the air-contact axis.

(A) LR developmental stages were quantified in cleared root samples. Significant differences were analyzed on a per-stage basis using Student's T-test ($P < 0.05$); statistically similar groups are indicated using same letter. (B, C, D) The *ProS32:erGFP* reporter is expressed in the protophloem and was used to mark the orientation of the diarch vascular cylinder with respect to the air-contact axis. Roots were imaged using a dissecting microscope and the distance between the two phloem-poles was quantified. A large relative distance measured between the two poles indicated that the xylem pole was oriented as in (B) while a small relative distance indicated that the xylem pole was oriented as in (D). The maximum and minimum distance values were used to calculate the midpoint distance, where the xylem pole would be oriented at a 45° angle with respect to the agar surface (C). (E) Measured distances were binned into two categories established by this midpoint ($n \geq 20$). No significant difference between the observed and expected distribution of values was observed based on Fisher's exact test, P-value < 0.05.

Fig. S6.

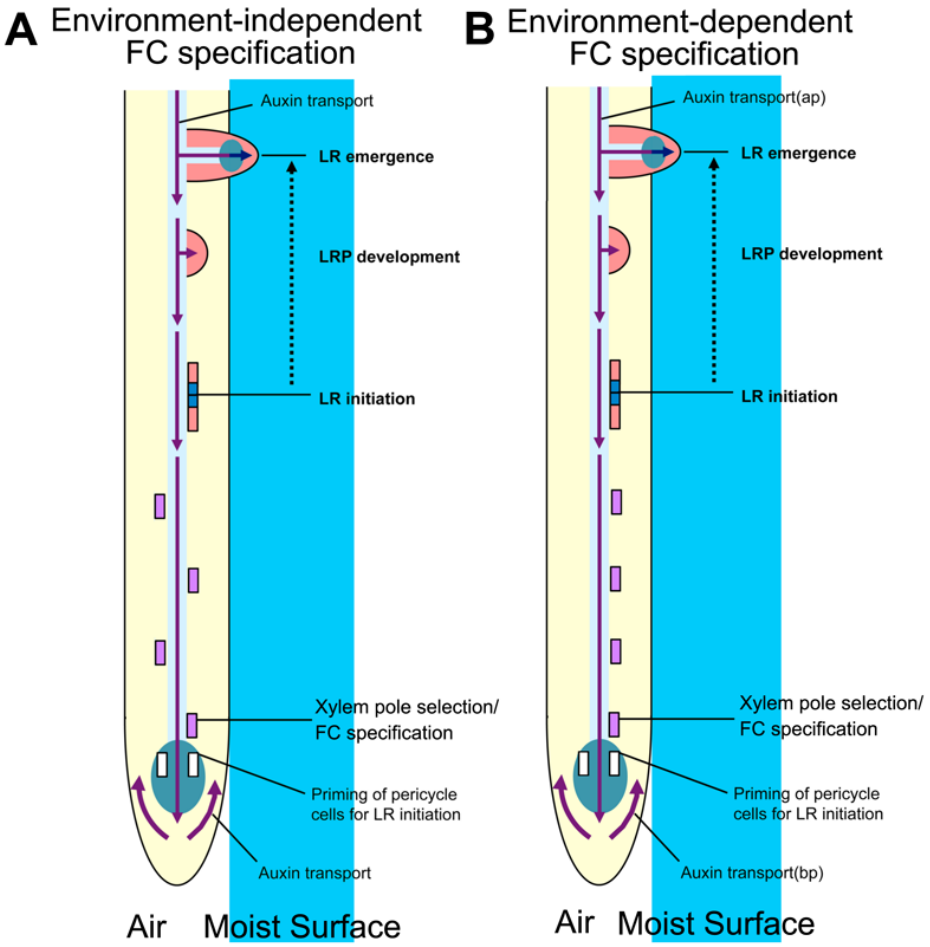

Fig. S6. Two models for lateral root patterning in Arabidopsis.
(A, B) Redrawn and modified from Fukaki and Tasaka (24). LR patterning begins at the root tip where a peak in auxin response leads to the priming of pericycle cells. Founder cells (FC) are specified in a subset of cells in the pericycle cell-layer overlying the xylem pole. At a later point in development, asymmetric anticlinal divisions are induced in the founder cells. Periclinal and anticlinal divisions continue and allow the LR primordia (LRP) to grow through the outer tissue layers of the primary root and emerge into the outside environment. (A) Diagram showing the environment-independent model for founder cell specification. Here, the xylem pole at which founder cells are specified is random or alternates between the two poles. This mechanism of patterning leads to founder cells being specified in regions of the root that are not permissive for later development. (B) In the environment-dependent model for founder cell specification, the external environment biases xylem-pole selection, thus most founder cells will be specified towards the permissive environment.

Fig. S7.

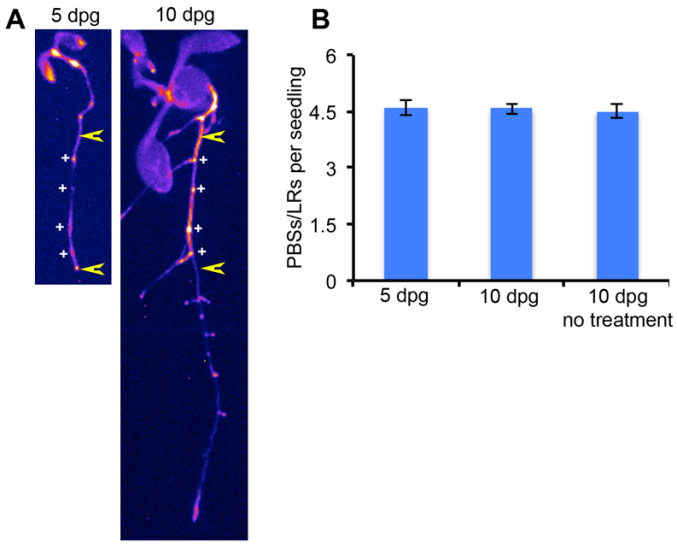

Fig. S7. PBSs are stably marked by *ProDR5:LUC+* reporter expression.
(A) We examined the persistence of *ProDR5:LUC+* reporter expression in PBSs. Regions of the root that formed between 3-5 days post-germination (dpg) were marked (region bracketed by yellow arrowheads) and the number of luminescent foci in this region was quantified after treatment with D-luciferin (B). Seedlings were allowed to grow for 5 more days and again treated with D-luciferin and imaged. The number of luminescent foci and emerged LR were quantified in the same region as before. No significant difference was observed between the two time points. To test whether D-luciferin treatment affected reporter expression, seedlings were marked at 3 and 5 dpg, but left untreated until day 10 at which point D-luciferin was applied and the roots imaged. As shown, a similar number of PBSs and LRs were observed. Error bars indicate SEM.

Fig. S8

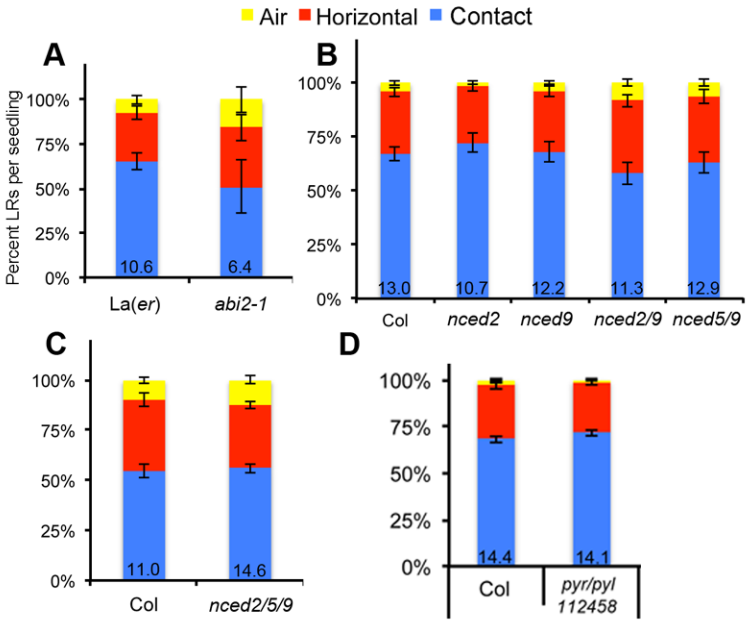

Fig. S8. ABA perception, signaling and biosynthesis pathways are not necessary for hydropatterning.
(A) The *abi2-1* mutant shows no significant differences in hydropatterning ($n \geq 8$). (B, C) The *NCED* genes perform the rate-limiting step in ABA biosynthesis, but have no effect on hydropatterning when mutated ($n \geq 25$). (D) The *pyr/pyl 112458* mutant has normal hydropatterning ($n \geq 20$). Average number of LRs per seedling shown at base of columns in bar charts. Error bars indicate SEM.

Fig. S9

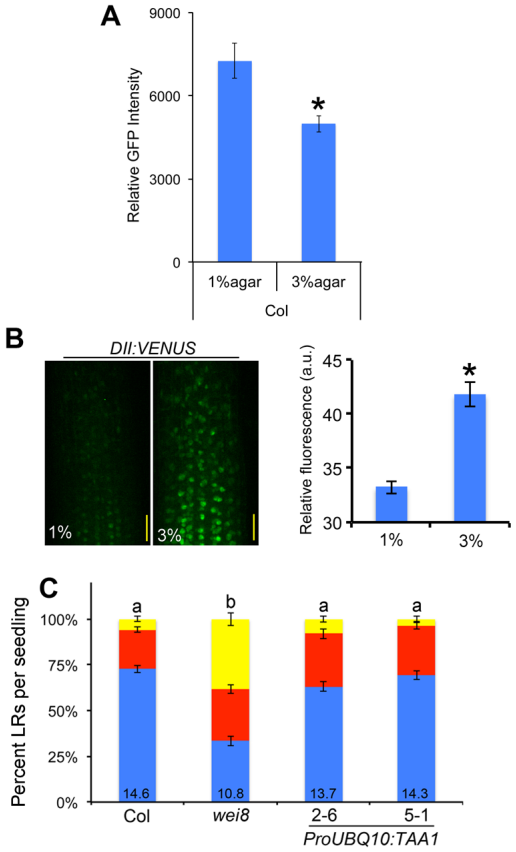

Fig. S9. Auxin reporter activity is moisture regulated. Effects of *TAA1* misexpression. (A) *ProDR5:erGFP* reporter activity in a wild-type (Col) roots grown on media containing 1% or 3% agar and quantified in the LRC and epidermis ($n \geq 8$). (B) The *DII-VENUS* reporter shows increased intensity in the meristem and elongation zone of roots grown on high agar-density media ($n = 11$). (C) The *ProUBQ10:TAA1* transgene is able to rescue the *wei8* hydropatterning defects. Average number of LRs per seedling shown at base of columns in bar charts. Error bars indicate SEM. Significant differences based on Fisher's exact test ($P < 0.05$) with similar groups indicated using same letter (C) or Student's T-test ($P < 0.05$) with significant differences labeled with asterisk (A, B). Scale bars = 50 μm.

Fig. S10

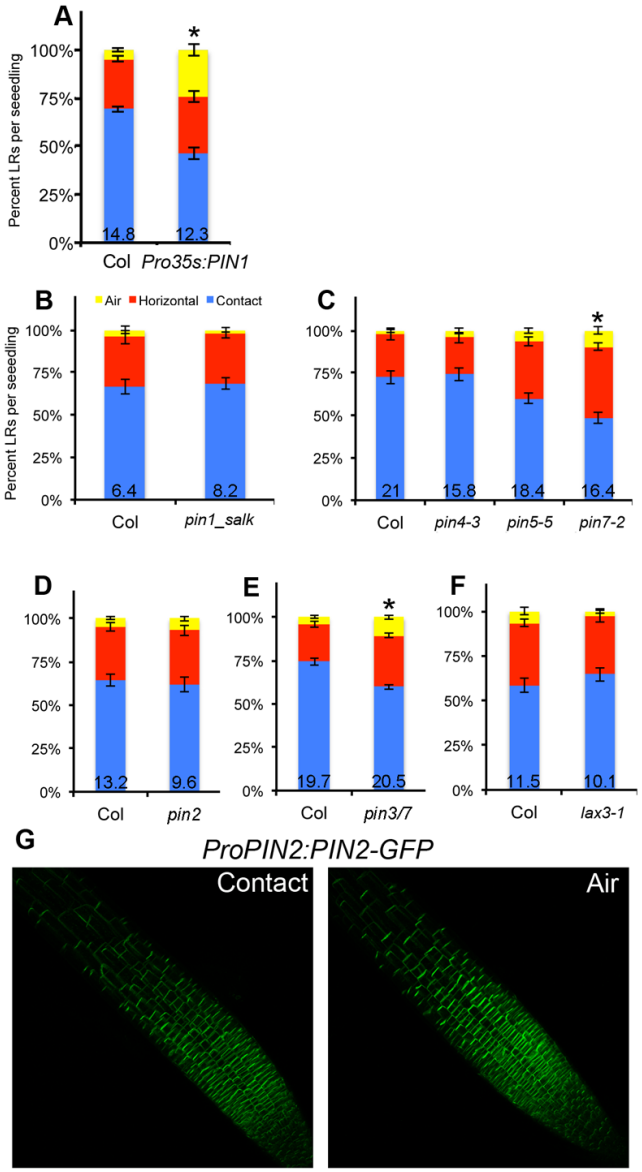

Fig. S10. Effects of changes in PIN transporter activity on hydropatterning.
(A) *Pro35S:PIN1* roots showed defects in hydropatterning ($n \geq 20$). The *pin1* (B), *pin4*, *pin5* (C), *pin2* (D) and *lax3* (F) mutants have no effect on hydropatterning. The *pin7* (C) and *pin3/7* (E) mutants cause a modest defect. Average number of LRs per seedling shown at base of columns in bar charts. (G) Maximum intensity projection of a confocal image stack of the *ProPIN2:PIN2*-GFP, which does not show obvious differences in expression pattern between the contact and air sides. Error bars indicate SEM. Asterisk marks significant differences based on Fisher's exact test, P-value < 0.05.

Supporting Information

Bao et al. 10.1073/pnas.1400966111

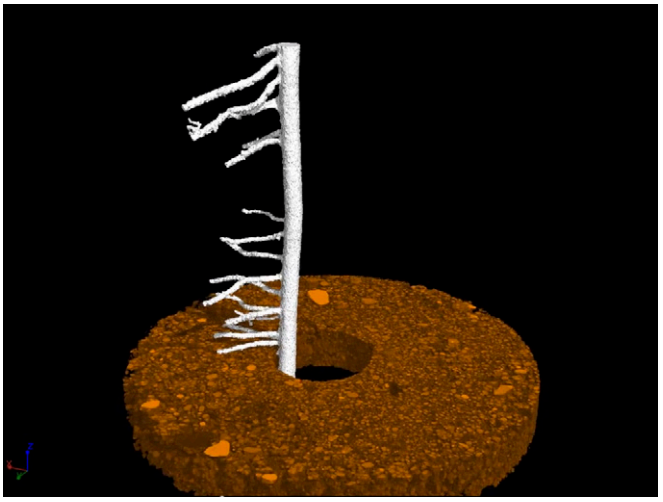

Movie S1. MicroCT 3D volume reconstruction of maize root growing through a soil macropore. Root is in partial contact with the soil and exhibits lateral root hydropatterning.

Movie S1

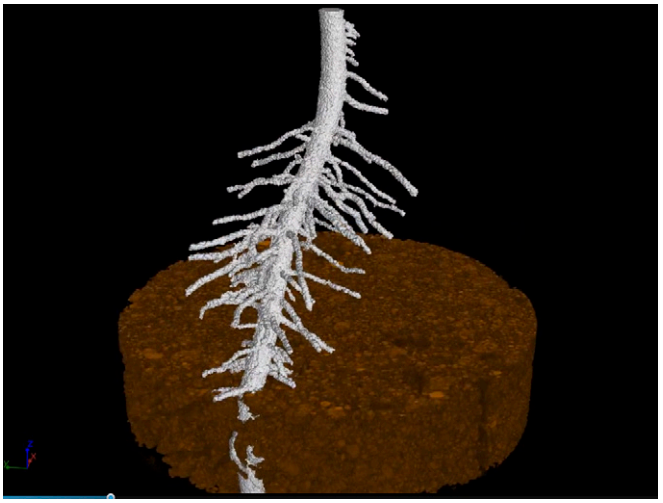

Movie S2. MicroCT 3D volume reconstruction of maize root growing through soil. Primary root is in contact with the soil on all sides. Lateral root development occurs around the entire circumferential axis of the primary root.

Movie S2

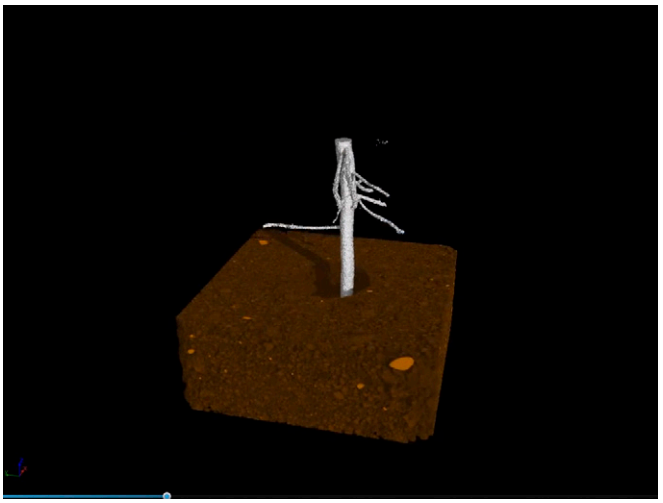

Movie S3. MicroCT 3D volume reconstruction of maize root growing through a soil macropore but with no contact. Root develops sporadic lateral roots in all directions.

Movie S3

Other Supporting Information Files

SI Appendix (PDF)